Chemical Structure and Nonlinear Optical Properties of Polar Self-Assembling Films

Leiming Li, Eugene R. Zubarev, Brad A. Acker, and Samuel I. Stupp*

Departments of Materials Science and Engineering and Chemistry, Medical School, Northwestern University, Evanston, Illinois 60208

Received May 7, 2001; Revised Manuscript Received November 5, 2001

ABSTRACT: We report on the influence of molecular chemical structure on second harmonic activity in several homologous series of self-assembling short chain polymers containing both molecularly rigid and flexible segments and known to form supramolecular nanostructures. The second-order nonlinear optical susceptibility and physical structure of films formed by these molecules were investigated by second harmonic generation experiments and small-angle X-ray scattering. It was observed that all series of molecules formed polar films with a layered structure by self-assembly. The nonlinear susceptibilities were found to increase with the ratio of first hyperpolarizability to layer period in the self-assembled films, further suggesting spontaneous polar order in these layers of supramolecular structures.

Introduction

A family of triblock molecules was previously synthesized in our laboratory and found to possess the ability to self-organize into supramolecular nanostructures of molecular thickness which in turn organize further into layer structures.[1−4] These molecules have "rod−coil" architecture, containing a molecularly rigid rod-like molecular segment covalently attached to a flexible coil-like segment. The coil segment is itself a diblock structure, containing one segment with large cross section units and a second one with smaller cross section units bonded to the crystallizable rod-like segment. All these structural details are thought to be a key factor in the nature of their self-assembling behavior. Here we collect further evidence for the noncentrosymmetric mushroom-shaped nature of the nanostructures formed by these molecules and also for polar organization in the films they form. Polar structure is the origin of many important properties of materials such as second-order nonlinear optical activity, piezoelectricity, ferroelectricity, and creating films with two chemically different parallel surfaces. The molecules studied here differ in the chemical structure of their crystallizable rod-like segments.

Nonlinear optical behavior of bulk organic materials is determined by both the molecular hyperpolarizability and the spatial arrangement of molecules in media.[5−8] It is well-known that dipolar second harmonic generation (SHG) signals are observed in organic films containing molecules with donor and acceptor groups connected by a conjugated segment and organized in noncentrosymmetric fashion.[9−11] One of the most common methods to achieve this polar arrangement is to align molecules in an electric field.[12−15] Thus, nanomushrooms formed by parallel aggregation of molecules could give rise to SHG signals if self-organized into polar structures. In this paper we have measured SHG response in the unpoled films. Short chain triblock polymers **1a**−**1d** contain oligostyrene and oligobutadiene coils with biphenyl ester rod segments of various lengths terminated by trifluoromethyl groups. Structures **2a** and **2b** have the same oligostyrene−oligoisoprene coil segments, but the biphenyl ester segment of **2a** is substituted by donor (amino) and acceptor (nitro) groups. Structures **3a** and **3b** also have the same oligostyrene−oligoisoprene coil segments but different rod segments that contain conjugated phenylenevinylene segments. We have also studied here the SHG activity of the self-assembling films **2b** with the addition of small chromophores **4**. All chemical structures studied are shown in Figure 1.

Experimental Section

Synthesis. Molecules **1a**−**1d** were prepared from hydroxyl-terminated rod−coils that were previously described.[1] The hydroxyl-terminated rod−coils were coupled with *p*-trifluoromethylbenzoic acid under the same esterification conditions used for the synthesis of OH-terminated molecules. The synthesis of **2a** and **4** can be found in ref 17, and the syntheses of **2b**,[1] **3a**, and **3b**[4] were previously reported.

Sample Preparation. Films of **1a**−**1d** were prepared by dissolving these materials in chloroform and casting the saturated solutions between a cleaned cover glass and an octadecyltrichlorosilane (OTS)-plated cover glass to form wedge samples. At one end a 100 μm thick Teflon spacer was placed between the two glasses, and at the other end the two glasses were pressed firmly together. This way a 1.8 cm long and 0.6 cm wide wedge-shaped space was defined for chloroform solutions. The samples were left in air for 48 h to allow the solvent to evaporate slowly from the wedge and then allowed to dry further under vacuum of about 0.01 atm for another 48 h. As the solvent evaporated, a solid strip formed at the edge of the substrate, about 0.1 cm wide and 1.8 cm long. Solidification began where the two glasses contacted and extended to the spacer at the other end. Figure 2 shows schematically the top and side views of a wedge sample after the solvent has evaporated. The dark arrow in Figure 2 represents the measuring path and direction for film thickness and SHG signals, and both measurements were obtained from the same measuring points along the path. Films of **2a**, **2b**, **3a**, and **3b** were prepared by casting the corresponding saturated chloroform solution onto a glass substrate. Particular care was taken to prepare films with a wide variation in thickness across the diameter of the films in order to obtain wedge fringes (SHG intensity vs sample thickness), and measurements of thickness and SHG were also obtained from the same measuring points on the films. The procedure used to prepare

* To whom correspondence should be addressed. This work was mostly carried out at the University of Illinois at Urbana−Champaign.

10.1021/ma010793p CCC: $22.00
Published on Web 02/21/2002

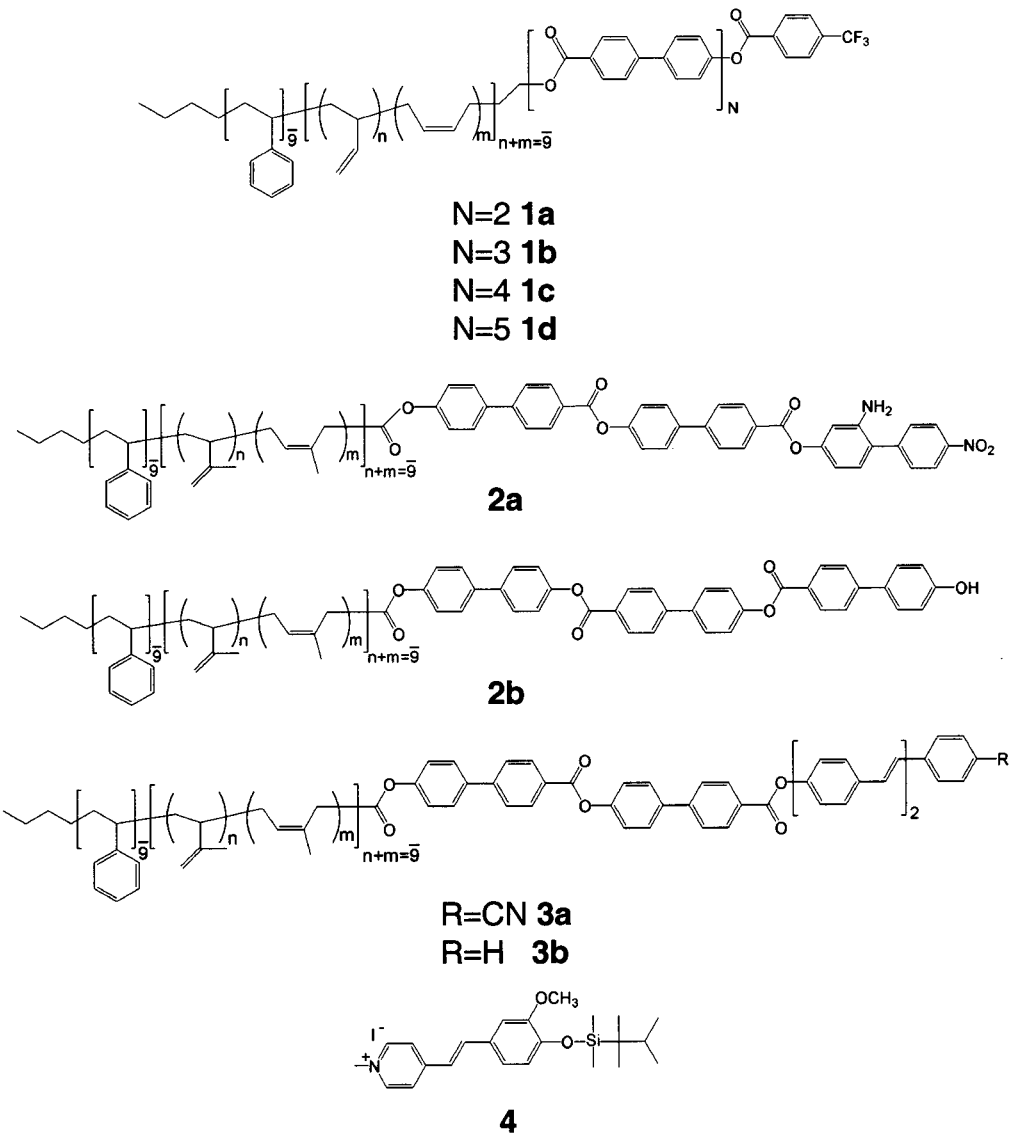

Figure 1. Chemical structures of the molecules studied.

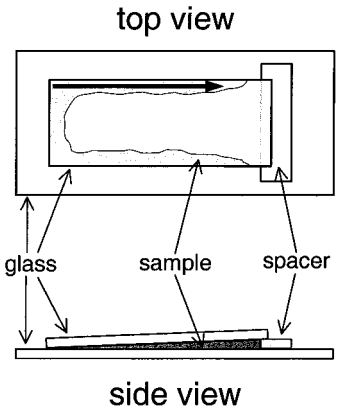

Figure 2. Schematic of a wedge sample with top and side views. The dark filled arrow indicates the path and direction of film thickness and SHG measurements.

these films is described elsewhere.[2] Films containing chromophores **4** were prepared by dissolving molecules **2b** in chloroform to form a 2 wt % solution, to which **4** was added to prepare three solutions with different molar ratio of **2b** to **4**, 1:1, 3:1, and 10:1. Thin films were prepared from each solution by casting on glass substrates and drying in air for 2 days. The films were visually smooth and had thickness in the order of several microns.

Film Characterization. The thickness profiles for the films cast on glass substrates were measured using a Sloan Dektak3-ST surface profilometer. The locations of the profilometer scanning paths across each film were recorded by applying small dots of ink onto the back of the glass substrates to mark the beginning and ending points of the scanning paths. Cast and dried thin films were scratched off glass substrates and grounded into powders for small-angle X-ray scattering (SAXS) measurements. SAXS was carried out on a Siemens Anton Paar high-resolution small-angle camera equipped with a Hi-Star area detector and Bruker (Siemens) SAXS software mounted on an M18X-HF22 SRA rotating anode generator. Powder diffraction rings were integrated over 360° to yield the patterns and were calibrated using a silver behenate standard.

Nonlinear Optics. Samples were mounted onto a rotation/translation stage, and the p-polarized (electric field of the laser beam in the incident plane) or s-polarized (electric field perpendicular to the incident plane) laser beam was tightly focused onto the sample areas, yielding a peak intensity of up to 30 MW/cm^2. The 1064 nm fundamental beam was produced by a Q-switched Nd:YAG laser with a 20 ns pulse width operating at a 20 Hz repetition rate. The transmitted second harmonic generation at 532 nm was separated from the fundamental via a series of green pass filters and a monochromator and collected by a photomultiplier tube (PMT). The signal was then sent into a digital data acquisition system. Figure 3 shows schematically the incident laser beam used in

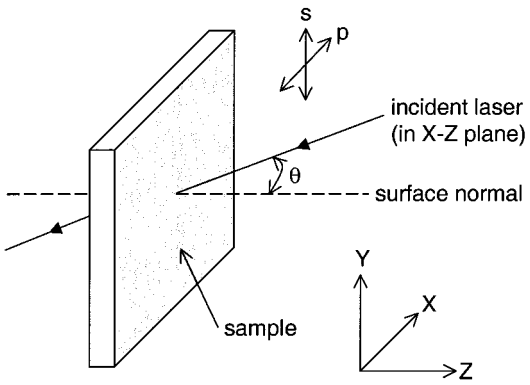

Figure 3. Schematic representation showing the incident laser electric field polarization for SHG experiments. The plane of incidence lies in the $X-Z$ plane, θ is the incident angle, and *p* and *s* represent parallel and perpendicular polarizations, respectively, of the laser with respect to the incident plane.

SHG measurements. Maker fringes (SHG intensity vs incident angle)[16] and wedge fringes (SHG intensity vs sample thickness) were both obtained for thin film samples. To obtain Maker fringes, the incident angles of the laser beam with either p- or s-polarization were continuously changed by rotating the sample about the *Y*-axis (through the incident point on the sample surface). For wedge fringes, the incident angle was fixed (45°) while the sample moved horizontally (along *X*-axis) to continuously change the sample thickness probed by a laser beam with p-polarization.

Results and Discussion

SAXS patterns obtained from the powder samples revealed strong (001) peaks for all self-assembling materials investigated. Upon annealing, materials **1a**−**1d**, **2b**, and **3a** showed (002) peaks as well. The layer thickness values obtained from the corresponding (001) peaks were 67, 81, 95, and 97 Å for **1a**, **1b**, **1c**, and **1d** films, respectively, 79 and 70 Å for **2a**[17] and **2b**,[1] and 78 and 77 Å for **3a** and **3b** films.[4] These values corresponded roughly to the length of one average-size triblock molecule as calculated by the molecular modeling program SYBYL. Therefore, SAXS results indicate that films formed by these self-assembling molecules have a layered structure.

The relation between the square root of the transmitted second harmonic intensity $I_{2\omega}$ and $\chi^{(2)}_{\text{eff}}$, the effective second-order nonlinear optical susceptibility, can be written as follows:[18]

$$\sqrt{I_{2\omega}} = C\chi^{(2)}_{\text{eff}} t_\omega^2 \sqrt{T_{2\omega}}\, p(\theta) \frac{I_\omega}{n_{2\omega}^{\,2} - n_\omega^{\,2}} \sin\left[\frac{2\pi L}{\lambda_\omega}(n_\omega \cos\theta_\omega - n_{2\omega}\cos\theta_{2\omega})\right] \quad (1)$$

where C is a constant, $\chi^{(2)}_{\text{eff}}$ is the effective second-order bulk susceptibility describing macroscopic nonlinear properties of films, θ is the angle of incidence, and n_ω and $n_{2\omega}$ are the refractive indices for the fundamental beam and the second harmonic beam, respectively. In the materials of interest, t_ω and $T_{2\omega}$ are the corresponding transmission factors, $p(\theta)$ is a projection factor, I_ω is the power of the incident fundamental laser beam, and L is the thickness of the sample.

Experimental results from SHG intensity measurements suggest that bulk films possess polar ∞mm symmetry. When samples were rotated about the film surface normal, no obvious changes in optical properties were observed, so the normal was assumed to be the ∞-fold axis. The Maker fringes shown in Figure 4 for sample **1b** with either p- or s-polarized incident fundamental laser are consistent with these films having polar ∞mm symmetry since SHG intensities would be canceled as explained in eq 1 when $\theta = 0°$ (normal incidence).[18] Similar Maker fringes were observed for other samples **1a**, **1c**, and **1d** in the first group, **2a** and **2b** in the second group, and **3a** and **3b** in the third group of molecules. Therefore, considering the layered structure revealed by SAXS mentioned above, all rod−coil molecules studied here tend to self-assemble into polar lamellar films.

Figure 5 shows curves for SHG intensities as a function of sample thickness (wedge fringes) corresponding to materials **1a**−**1d**. The same SHG intensity scale was used for all four materials. These curves were obtained by scanning a p-polarized laser beam with an incident angle of 45° along the center of wedge sample strips (schematic shown in Figure 2) whose thickness changed linearly from approximately 0 up to 60 μm (as measured by the surface profilometer). The theoretical curves (solid lines) can be described by eq 1. As

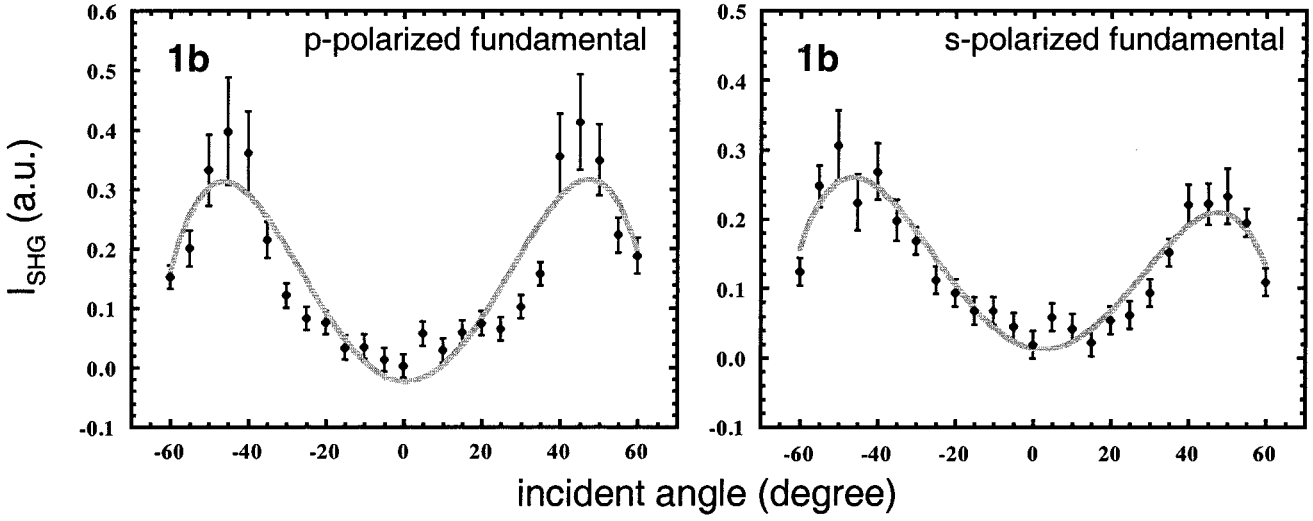

Figure 4. Maker fringes of self-assembling films composed of molecules **1b** obtained with a p-polarized and a s-polarized fundamental laser beam.

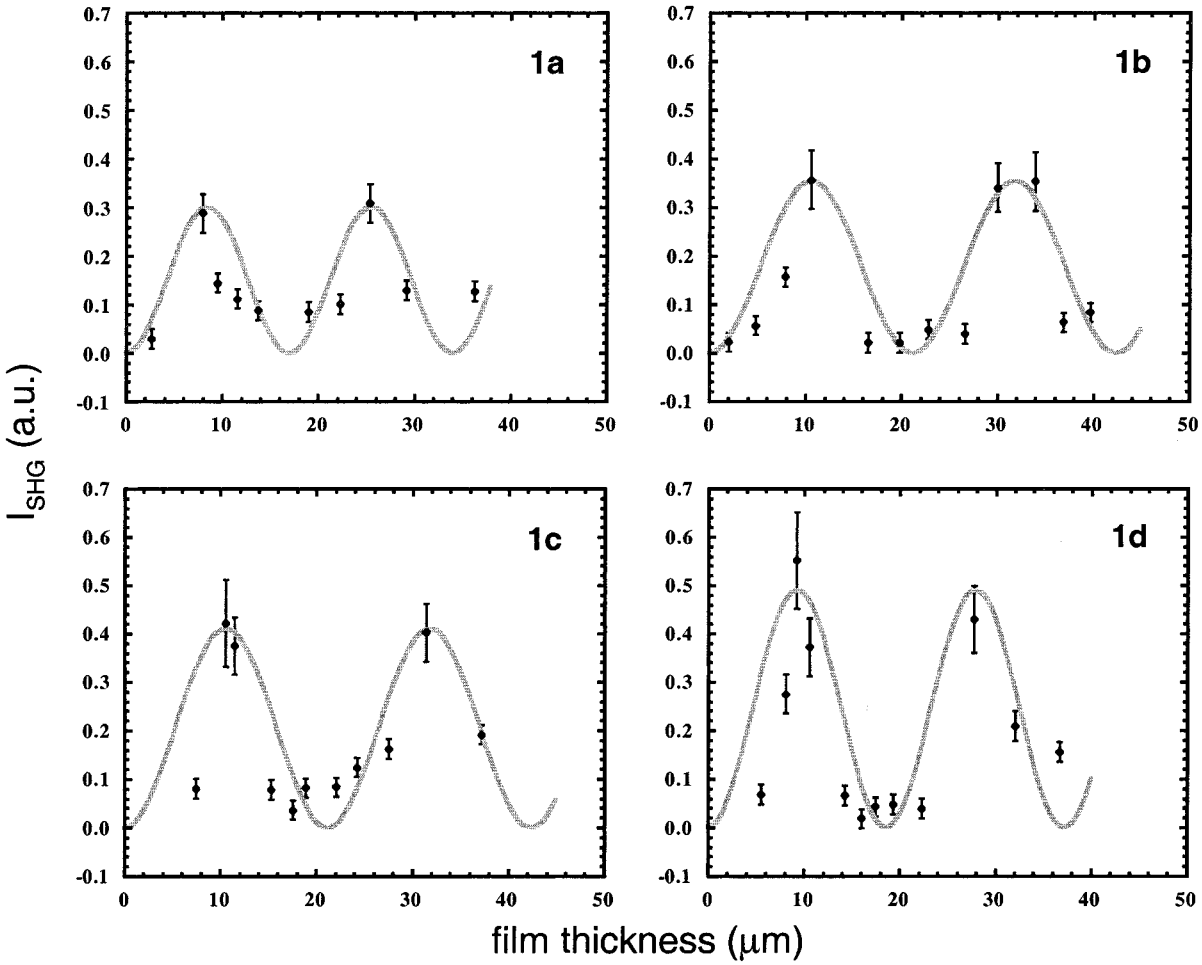

Figure 5. Wedge fringes for films composed of molecules **1a**, **1b**, **1c**, and **1d**. The solid curves are calculated using eq 1 (see text).

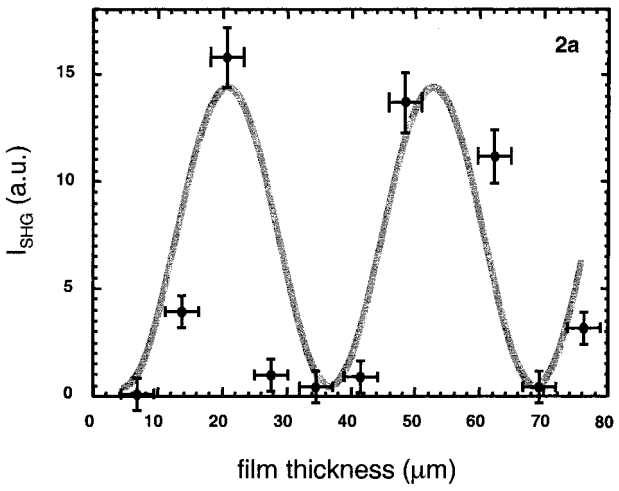

Figure 6. Wedge fringes for films composed of molecules **2a**.

mentioned above, films of materials **1a**−**1d** were produced between a hydrophilic glass and a hydrophobic OTS surface inside a wedge. We thought that this difference in chemistry between opposite wedge surfaces would enhance polar self-assembly. However, similar results were obtained between symmetric glass surfaces. Wedge curves were also obtained for materials **2a** (shown in Figure 6), **2b**, **3a**, and **3b** that formed films on glass with a wide variation in thickness. To estimate the SHG intensities contributed by interfaces (substrate−sample and sample−air interfaces), we prepared very thin films, whose thicknesses corresponded to ∼10 or less self-assembling molecular layers and were much thinner than those of the wedge films. Compared with the wedge films, the maximum SHG signals we could obtain from the thin films were within noise levels when they were excited with the same fundamental laser intensity. Therefore, the SHG signals should originate mostly from the bulk of samples.

We analyzed SHG data in molecules **1a**−**1d** in order to understand the effect of chemical structure. It is clear from Figure 5 that as the number of biphenyl groups increases from 2 to 5 in the molecules of materials **1a** to **1d**, the corresponding SHG intensities increase as well. As stated before, the incident angle θ and the fundamental beam power I_ω were kept the same for all samples **1a**−**1d** when measuring the wedge curves, and their $\chi^{(2)}_{eff}$ values were calculated using eq 1 from the SHG intensities at their first peak where $L = L_c$, the coherent length of the films, and where the sine term in eq 1 goes to unity. We develop a model below to help us understand the effect on SHG of biphenyl ester repeats in the rod segments that drive self-assembling behavior. For p-polarized incident fundamental laser beam and p-polarized second harmonic light generated from films with polar ∞mm structure,[8]

$$\chi^{(2)}_{eff} = 3\chi^{(2)}_{zxx} \sin\theta \cos^2\theta + \chi^{(2)}_{zzz} \sin^3\theta \qquad (2a)$$

where θ is the incident angle, and $\chi^{(2)}_{zxx}$ and $\chi^{(2)}_{zzz}$ are the only two nonvanishing elements of the $\chi^{(2)}$ tensor considering Kleinman symmetry. For a rod-shaped

molecule whose charge transfer occurs along molecular axis, β_{zzz} is often the dominant component of molecular hyperpolarizability β describing the molecular second-order nonlinear optical properties of the chromophores. The relation between macroscopic susceptibilities $\chi^{(2)}$ and microscopic hyperpolarizability β is given by[19]

$$\chi^{(2)}_{zzz} = N\beta_{zzz}f\langle\cos^3\phi\rangle \tag{2b}$$

$$\chi^{(2)}_{zxx} = 0.5N\beta_{zzz}f\langle\sin^2\phi\cos\phi\rangle \tag{2c}$$

where N is the density of chromophores in the film, f represents the local field factors, and ϕ is the tilt angle of the molecular axis away from the substrate surface normal. Combining eqs 2a, 2b, and 2c,

$$\chi^{(2)}_{\text{eff}} \propto N\beta_{zzz} \tag{2d}$$

Equation 2d relates approximately $\chi^{(2)}_{\text{eff}}$ with molecular microscopic nonlinearities if local field factors and molecular tilt angle distributions of the polar ∞mm films are treated as constants.

The molecules within the same group have different lengths but very similar average cross section areas. Thus, the molecular density of each film is inversely proportional to the thickness of the molecular layers, d, determined by SAXS,

$$N \propto \frac{1}{d} \tag{3}$$

Combining eqs 2d and 3, one can state that

$$\chi^{(2)}_{\text{eff}} \propto \frac{\beta_{zzz}}{d} \tag{4}$$

Since coil segments in all molecules studied are not conjugated, we assume that they do not contribute to the magnitude of β_{zzz}. The magnitude of β_{zzz} was calculated for each molecule using ZINDO (method: TDA; model Hamiltonian: INDO/1) included in the quantum mechanics computational program Cerius2. These calculations indicated that β_{zzz} was indeed much larger than all other hyperpolarizabilty components in the molecules studied. $\chi^{(2)}_{\text{eff}}$ and β_{zzz}/d are plotted and compared within each group of materials in Figure 7. Interestingly, for materials **1a**−**1d**, as the number of biphenyl groups increases from 2 to 5, both $\chi^{(2)}_{\text{eff}}$ and β_{zzz}/d increase, supporting a close relation between these two parameters. Similar results are observed for materials **2a** and **2b** (see Figure 7b) and materials **3a** and **3b** as well (see Figure 7c). The $\chi^{(2)}_{\text{eff}}$ data and the fringes obtained are important not only because they clearly demonstrate the key role played by the chemical structure of rod segments but also because they demonstrate that polar self-assembly in bulk is behind the SHG signals observed.

We also probed in this paper the effect of adding a chromophore (structure **4** in Figure 1) to one of our self-assembling systems that form films with net polarity. The concept explored here was the spontaneous alignment of the chromophores in the polar self-assembling medium. For mixtures of **2b** and **4** the p-polarized laser beam with an incident angle of 45° was used to obtain the effective second-order susceptibility $\chi^{(2)}_{\text{eff}}$ for various concentrations of **4**. Maker fringes were measured in a

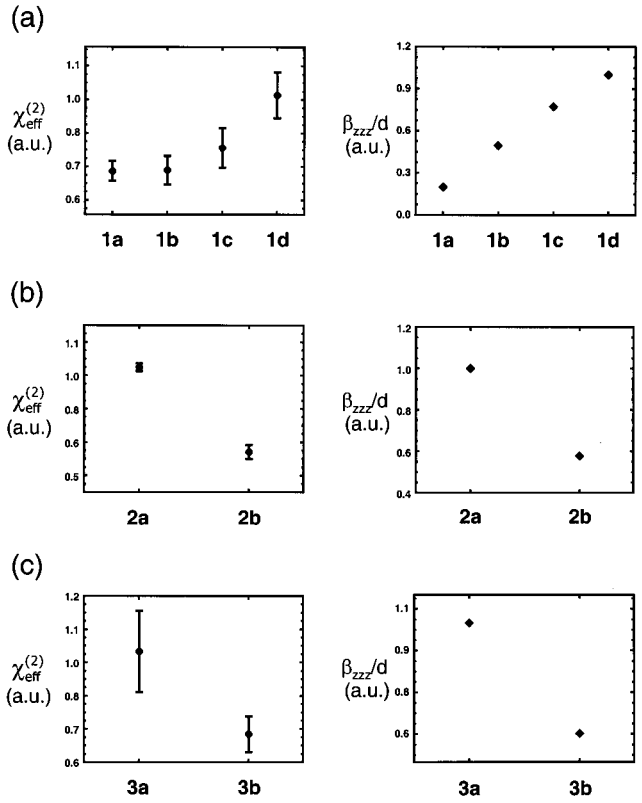

Figure 7. Plots of $\chi^{(2)}_{\text{eff}}$ and β_{zzz}/d for materials **1a**, **1b**, **1c**, **1d** (a), **2a**, **2b** (b), and **3a**, **3b** (c).

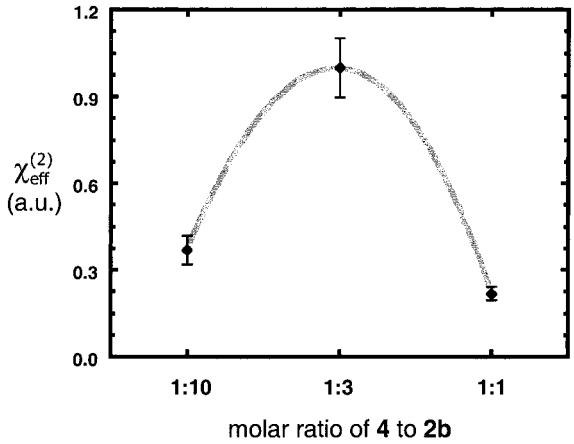

Figure 8. Plot of $\chi^{(2)}_{\text{eff}}$ for hybrid films composed of **2b** and three different molar ratios of **4** to **2b**, 1:10, 1:3, and 1:1.

way similar to that described before. Figure 8 shows the change of $\chi^{(2)}_{\text{eff}}$ as the molar ratio of **4** to **2b** increases in samples. First of all, the $\chi^{(2)}_{\text{eff}}$ value for films of **2b** was found to be much smaller than the susceptibilities of films containing mixture of **2b** and **4**, approximately 0.02 in the scale of Figure 8. Second, the hybrid material with an approximate molar ratio of 1:3 produces the largest effective second-order susceptibility $\chi^{(2)}_{\text{eff}}$, and as the concentration of chromophore molecules **4** increases beyond 1:3, the susceptibility begins to decrease. The decrease might be related to the aggregation of chromophores at high concentrations that changes their electronic structures and susceptibilities.[20−23] Alternatively, aggregates of chromophores might form centrosymmetric structures that are not SHG active. However, the hybrid films retain their polar ∞mm symmetry for all three ratios, suggested by Maker

fringes generated from all of the films. On the basis of our results, we believe that chromophore molecules **4** acquire polar orientation in the matrix with net polarity formed by materials **2b**.

Conclusions

We have reported here on three sets of architecturally similar but chemically different molecules that self-assemble into macroscopically polar films. The $\chi^{(2)}_{eff}$ values were found strongly influenced by molecular hyperpolarizability and the characteristic layer spacing of these self-assembling materials containing triblock molecules. These results demonstrate how bulk nonlinear optical properties and other related physical properties can be tailored through supramolecular chemistry.

Acknowledgment. The work was supported by grants from the Department of Energy (DE-FG02-00ER45810) and the National Science Foundation (DMR-9996253). The authors also acknowledge use of the Laser Laboratory of the Materials Research Laboratory and the Visualization Laboratory of the Beckman Institute for Advanced Science and Technology, both at the University of Illinois at Urbana−Champaign.

References and Notes

(1) Stupp, S. I.; LeBonheur, V.; Walker, K.; Li, L. S.; Huggins, K. E.; Keser, M.; Amstutz, A. *Science* **1997**, *276*, 384.
(2) Tew, G. N.; Li, L. M.; Stupp, S. I. *J. Am. Chem. Soc.* **1998**, *120*, 5601.
(3) Zubarev, E. R.; Pralle, M. U.; Li, L.; Stupp, S. I. *Science* **1999**, *283*, 523.
(4) Tew, G. N.; Pralle, M. U.; Stupp, S. I. *J. Am. Chem. Soc.* **1999**, *121*, 9852.
(5) Singer, K. D.; Kuzyk, M. G.; Sohn, J. E. *J. Opt. Soc. Am. B* **1987**, *4*, 968.
(6) Blum, R.; Sprave, M.; Sablotny, J.; Eich, M. *J. Opt. Soc. Am. B* **1998**, *15*, 318.
(7) Eaton, D. F. *Science* **1991**, *253*, 281.
(8) Prasad, P. N.; Williams, D. J. *Introduction to Nonlinear Optical Effects in Molecules and Polymers*; John Wiley & Sons: New York, 1991.
(9) Oudar, J. L. *J. Chem. Phys.* **1977**, *67*, 446.
(10) Lee, C.; Haas, D.; Man, H. T.; Mechensky, V. *Photonics Spectra* **1989**, *23*, 169.
(11) Lupo, D.; Prass, W.; Scheunemann, U.; Laschewsky, A.; Ringsdorf, H.; Ledoux, I. *J. Opt. Soc. Am. B* **1988**, *5*, 300.
(12) Mortazavi, M. A.; Knoesen, A.; Kowel, S. T.; Higgins, B. G.; Dienes, A. *J. Opt. Soc. Am. B* **1989**, *6*, 733.
(13) Meredith, G. R.; VanDusen, J. G.; Williams, D. J. *Macromolecules* **1982**, *15*, 1385.
(14) Singer, K. D.; Sohn, J. E.; Lalama, S. J. *Appl. Phys. Lett.* **1986**, *49*, 248.
(15) Williams, D. J. *Angew. Chem., Int. Ed. Engl.* **1984**, *23*, 690.
(16) Maker, P. D.; Terhune, R. W.; Nisenoff, M.; Savage, C. M. *Phys. Rev. Lett.* **1962**, *8*, 21.
(17) Acker, B. A. M.S. Thesis, University of Illinois at Urbana−Champaign, 1997.
(18) Jerphagnon, J.; Kurtz, S. K. *J. Appl. Phys.* **1970**, *41*, 1667.
(19) Eich, M.; Sen, A.; Looser, H.; Bjorklund, G. C.; Swalen, J. D.; Twieg, R.; Yoon, D. Y. *J. Appl. Phys.* **1989**, *66*, 2559.
(20) Robinson, B. H.; Dalton, L. R. *J. Phys. Chem. A* **2000**, *104*, 4785.
(21) Hayden, L. M. *Phys. Rev. B* **1988**, *38*, 3718.
(22) Schildkraut, J. S.; Penner, T. L.; Willand, C. S.; Ulman, A. *Opt. Lett.* **1988**, *13*, 134.
(23) Xu, Z.; Lu, W.; Bohn, P. W. *J. Phys. Chem.* **1995**, *99*, 7154.

MA010793P